BNL-224582-2023-TECH

C-A/AP/695

Estimates of the Recombination Rate for the Strong Hadron Cooling System in the EIC

G. Wang

June 2023

Collider Accelerator Department

Brookhaven National Laboratory

U.S. Department of Energy

USDOE Office of Science (SC), Nuclear Physics (NP) (SC-26)

DISCLAIMER

Estimates of the Recombination Rate for the Strong Hadron Cooling System in the EIC

G. Wang

Abstract

Monitoring the recombination process of the ions as they go through the cooling section serves as a crucial tool for aligning their energy with that of the electrons. In this note, we calculate the recombination rate for the Strong Hadron Cooling system based on the MBEC.

Introduction

The strong hadron cooling system for EIC consists of the modulator, the microbunching amplifier and the kicker section. In the modulator and the kicker section, the electrons are co-moving with the protons. If the relative velocity of an electron with respect to a proton is small enough, it can be captured by the proton and the resulting neutral particle, i.e. a hydrogen atom, will deviate from the designed trajectory and get lost around the cooling section. Since the probability of a proton capturing an electron depends on the relative velocity between them, one can align the energy of the two beams based on the number of hydrogen atoms detected by a recombination monitor. In this note, we estimate the rate at which the hydrogen atoms produced by the recombination process for the SHC in EIC.

Equations

The recombination rate is calculated from the following equation

$$R = \gamma^{-2} N_p N_{bunch} \frac{\sigma_{es}}{\sigma_{ps}} n_e \frac{L_{cool}}{L_{ring}} \alpha_r \, , \tag{1}$$

where γ is the relativistic energy factor of the electrons and the ions, N_p is the number of protons in a bunch, N_{bunch} is the number of the proton bunches in the storage ring, σ_{es} is the RMS bunch length of the electrons, σ_{ps} is the R.M.S. bunch length of the protons, n_e is the spatial density of the electrons in the lab frame, L_{cool} is the length of the cooling section, L_{ring} is the circumference of the proton storage ring,

$$\alpha_r = \frac{\int\limits_{-\infty}^{\infty} d^3 v_i d^3 v_e f_e\left(v_e\right) f_I\left(v_i\right) \left|\vec{v}_e - \vec{v}_i\right| \sigma\left(\left|\vec{v}_e - \vec{v}_i\right|\right)}{\int\limits_{-\infty}^{\infty} d^3 v_i d^3 v_e f_e\left(v_e\right) f_I\left(v_i\right)} \tag{2}$$

is the recombination rate coefficient averaged over the velocity distribution of the electrons and that of the ions with the recombination cross section given by

$$\sigma(v) = A\frac{2h\nu_0}{m_e v^2}\left[\ln\left(\sqrt{\frac{2h\nu_0}{m_e v^2}}\right) + \gamma_1 + \gamma_2\left(\frac{m_e v^2}{2h\nu_0}\right)^{1/3}\right], \tag{3}$$

where $A = 2.11\times10^{-22} cm^2$, $\gamma_1 = 0.1402$, $\gamma_2 = 0.525$, $h\nu_0 = Z^2\alpha^2 m_e^2/2 = Z^2\times13.6eV$, and $Z=1$ for protons. We assume that the transverse velocity distribution of both the electrons and that of the ions have the Gaussian profile, i.e.

$$f_e(v_e) = \frac{1}{2\pi\beta_{e,x}\beta_{e,y}}\exp\left(-\frac{v_{e,x}^2}{2\beta_{e,x}^2} - \frac{v_{e,y}^2}{2\beta_{e,y}^2}\right) f_{e,z}(v_{e,z}) \tag{4}$$

and the velocity distribution of the protons

$$f_I(v_i) = \frac{1}{2\pi\beta_{i,x}\beta_{i,y}}\exp\left(-\frac{v_{i,x}^2}{2\beta_{i,x}^2} - \frac{v_{i,y}^2}{2\beta_{i,y}^2}\right) f_{i,z}(v_{i,z}). \tag{5}$$

Since the longitudinal velocity spreads of the electrons and the ions in the co-moving frame are significantly smaller than the transverse velocity spreads, we assume that the longitudinal velocity spread is zero for this analysis, i.e.

$$f_{e,z}(v_{e,z}) = \delta(v_{e,z} - v_{z0}), \tag{6}$$

and

$$f_{i,z}(v_{i,z}) = \delta(v_{i,z}). \tag{7}$$

Inserting eq. (3)-(7) into eq. (2) and carrying out the integration (APPENDIX B) yields

$$\alpha_r = Ac\frac{h\nu_0}{m_e\beta_x\beta_y}\sqrt{\frac{2h\nu_0}{m_e c^2}}$$
$$\int_0^\infty \frac{1}{\sqrt{y + \frac{m_e v_{z0}^2}{2h\nu_0}}}\left[-\frac{1}{2}\ln\left(y + \frac{m_e v_{z0}^2}{2h\nu_0}\right) + \gamma_1 + \gamma_2\left(y + \frac{m_e v_{z0}^2}{2h\nu_0}\right)^{1/3}\right]\exp\left(-\frac{h\nu_0}{kT_1}y\right) I_0\left(\frac{h\nu_0}{kT_1}\eta\cdot y\right)dy, \tag{8}$$

where

$$kT_1 \equiv \frac{2m_e\beta_x^2\beta_y^2}{\beta_x^2 + \beta_y^2}, \tag{9}$$

$$\eta \equiv \frac{\beta_x^2 - \beta_y^2}{\beta_x^2 + \beta_y^2}, \tag{10}$$

$$\beta_x \equiv \sqrt{\beta_{i,x}^2 + \beta_{e,x}^2} \,, \tag{11}$$

and

$$\beta_y \equiv \sqrt{\beta_{i,y}^2 + \beta_{e,y}^2} \,. \tag{12}$$

Estimates of the recombination rate for the SHC in EIC

With the parameters listed in table 1 and expression given by eq. (8), the recombination rate coefficient is calculated and shown in fig. 1 (left). As a comparison, fig. 1 (right) shows the recombination rate coefficient calculated for the CeC experiment at RHIC with parameters assumed in table 2 (see APPENDIX A for the expression of calculating the recombination rate with round electron and ion beams). As shown in fig. 1, the recombination rate expected for the SHC in the EIC is about a factor of two lower than that in the CeC experiment. However, there are 1160 proton bunches in the EIC while there is only one hadron bunch in the CeC experiment, which may lead to significantly higher background noise for detecting the recombination signal in the SHC as compared to that of the CeC experiment.

Proton beam		Electron beam	
Energy, gamma	293.09	Energy, gamma	293.09
Horizontal emittance	11.3 nm	Horizontal norm. emittance	2.8 µm
Vertical emittance	1 nm	Vertical norm. emittance	2.8 µm
β_x at modulator	17.09 m	β_x at modulator	76.4 m
β_y at modulator	17.08 m	β_y at modulator	10.15 m
σ_{vx}/c at modulator (beam frame)	7.537E-3	σ_{vx}/c at modulator (beam frame)	3.277E-3
σ_{vy}/c at modulator (beam frame)	2.243E-3	σ_{vy}/c at modulator (beam frame)	8.992E-3
Energy spread	6.8E-4	Energy spread	1E-4
σ_{vz}/c at modulator (beam frame)	6.8E-4	σ_{vz}/c at modulator (beam frame)	1E-4
Population	6.9E10	Bunch charge	1 nC
RMS bunch length	6 cm	RMS bunch length	7 mm

Table 1: parameters used for the estimates of the recombination rate in the SHC of the EIC

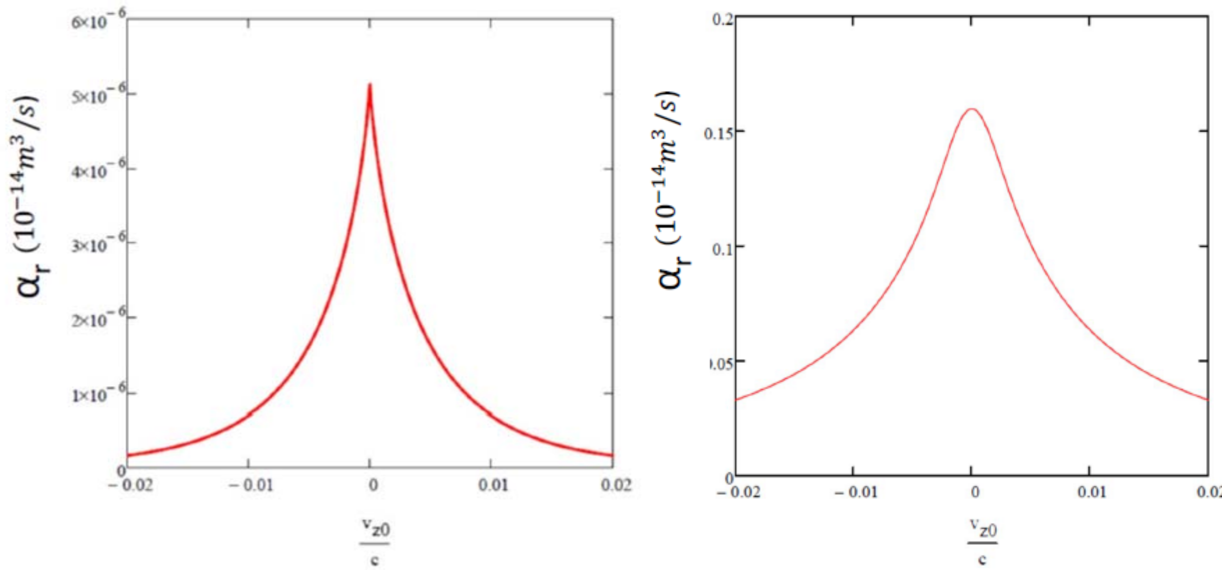

Figure 1: recombination coefficient as calculated for the SHC in EIC (left) and that for the CeC experiment (right). The abscissa is the longitudinal average velocity of the electrons with respect to the average velocity of the ions and the ordinate is the recombination rate coefficient, α_r, as defined in eq. (1).

Au beam		**Electron beam**	
Energy, gamma	28.5	Energy, gamma	28.5
Horizontal emittance	87.7 nm	Horizontal norm. emittance	3 µm
Vertical emittance	87.7 nm	Vertical norm. emittance	3 µm
β_x^* at cooling section	5 m	β_x at cooling section	2.3 m
β_y^* at modulator	5 m	β_y at modulator	2.3 m
σ_{vx}/c at modulator (beam frame)	4E-3	σ_{vx}/c at modulator (beam frame)	6.1E-3
σ_{vy}/c at modulator (beam frame)	4E-3	σ_{vy}/c at modulator (beam frame)	6.1E-3
Energy spread	1.3E-3	Energy spread	5E-4
σ_{vz}/c at modulator (beam frame)	1.3E-3	σ_{vz}/c at modulator (beam frame)	5E-4
Population	8.4E8	Bunch charge	1.5 nC
RMS bunch length	1.05m	RMS bunch length	3.6 mm

Table 2: Parameters used for the estimate of the recombination rate in the CeC experiment.

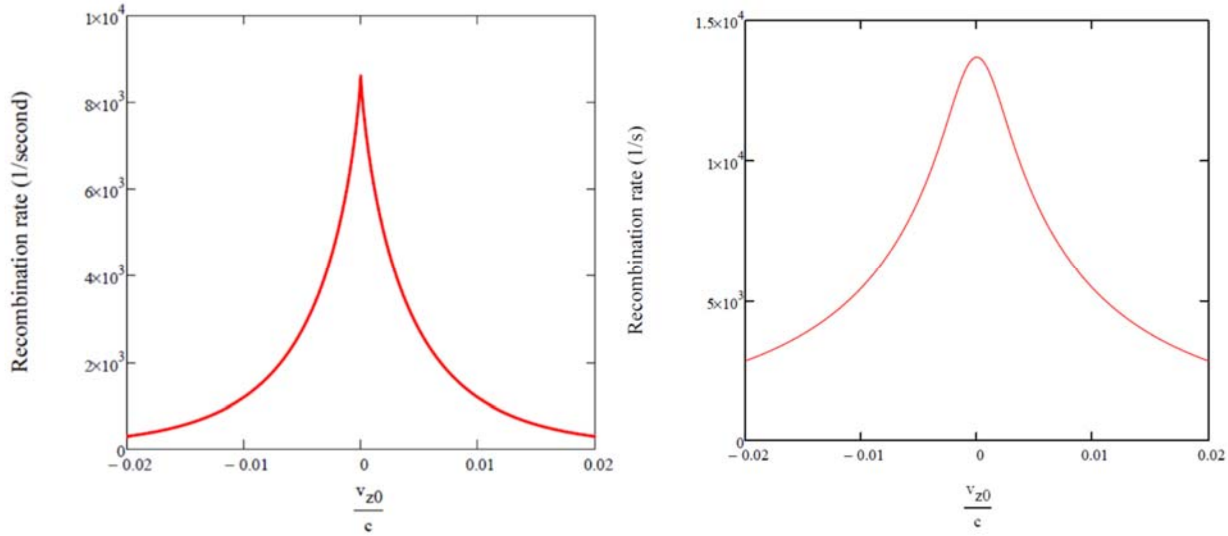

Figure 2: (left) The recombination rate as estimated from eq. (1) for the SHC in the EIC with the assumption of 35 meters of the cooling section and 1160 proton bunches; (right) the recombination rate as estimated for the CeC experiment at RHIC with the assumption of 1 Au bunch and 14 meters of the cooling section.

Au beam		Electron beam	
Energy, gamma	4.1	Energy, gamma	4.1
Horizontal emittance	385 nm	Horizontal norm. emittance	2.5 µm
Vertical emittance	385 nm	Vertical norm. emittance	2.5 µm
β_x^* at cooling section	25 m	β_x at cooling section	30 m
β_y^* at cooling section	25 m	β_y at modulator	30 m
σ_{vx}/c at modulator (beam frame)	5.2E-4	σ_{vx}/c at modulator (beam frame)	5.9E-4
σ_{vy}/c at modulator (beam frame)	5.2E-4	σ_{vy}/c at modulator (beam frame)	5.9E-4
Energy spread	5E-4	Energy spread	3E-4
σ_{vz}/c at modulator (beam frame)	5E-4	σ_{vz}/c at modulator (beam frame)	3E-4
Population	5E8	Bunch charge (1 bunch, 3nC for 30 bunches)	0.1 nC
RMS bunch length	3.3 m	RMS bunch length	3.6 mm

Table 3: Parameters used for the estimate of the recombination rate in the LEReC system.

Using eq. (A3) and the parameters of LEReC shown in table 3, we can also calculate the recombination rate for the Low Energy RHIC electron Cooling (LEReC). The recombination rate is shown in fig. 3.

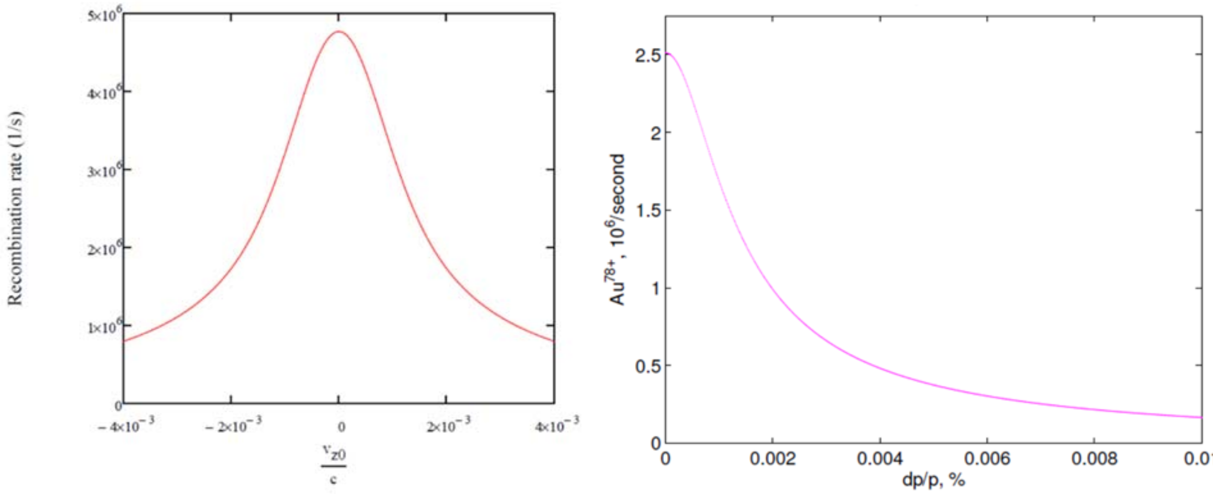

Figure 3: The recombination rate estimated for the LEReC as calculated from eq. (A3) (left) and that taken from [1](right). The factor of 2 difference between the two estimate comes from the difference in the current used in the estimate. The left plot assumes the peak current at the bunch center and the right plot is generated with averaging the electrons' current over the longitudinal bunch profile.

Summary

As shown in fig. 2, the recombination rate expected for the SHC in the EIC is about a factor of two lower than that in the CeC experiment. However, there are 1160 proton bunches in the EIC while there is only one hadron bunch in the CeC experiment, which may lead to significantly higher background noise for detecting the recombination signal in the SHC as compared to that of the CeC experiment. We also reproduced the results of the expected recombination rate for the LEReC system as estimated in C-A/AP/582 and confirmed that the estimated recombination rate for the SHC in the EIC will be 2~3 orders of magnitudes lower than that in the LEReC.

REFERENCES

[1] S. Zhang and M. Blaskiewicz, Recombination monitor, Report No. C-A/AP/582 (2017).

[2] G. Wang, arXiv: 2109.13980 (2021).

APPENDIX A: Expression for calculating the recombination rate with cylindrically symmetric electron beam and ion beam

For round electron beam and ion beam with Gaussian transverse velocity distribution, i.e.

$$f_e(v_e) = \frac{1}{(2\pi)^{3/2}\beta_{e,\perp}^2\beta_{e,z}}\exp\left(-\frac{v_{e,x}^2+v_{e,y}^2}{2\beta_{e,\perp}^2}\right)\exp\left(-\frac{(v_{e,z}-v_{z0})^2}{2\beta_{e,z}^2}\right), \tag{A1}$$

$$f_I(v_i) = \frac{1}{(2\pi)^{3/2}\beta_{i,\perp}^2\beta_{i,z}}\exp\left(-\frac{v_{i,x}^2+v_{i,y}^2}{2\beta_{i,\perp}^2}\right)\exp\left(-\frac{v_{i,z}{}^2}{2\beta_{i,z}^2}\right) \tag{A2}$$

with $\beta_{e,x}=\beta_{e,y}=\beta_{e,\perp}$ and $\beta_{i,x}=\beta_{i,y}=\beta_{i,\perp}$, eq. (2) can be reduced to [2]

$$\begin{aligned}\alpha_r = {} & \frac{Ach\nu_0}{kT_{ei}\eta}\sqrt{\frac{2h\nu_0}{m_e c^2}}\exp\left(\frac{m_e v_{z0}{}^2}{2kT_{ei}\eta^2}\right)\int_0^\infty\left(-\ln y+\gamma_1+\gamma_2 y^{2/3}\right)\exp\left(-\frac{h\nu_0}{kT_{ei}}y^2\right) \\ & \times\left\{Erf\left[\eta\sqrt{\frac{h\nu_0}{2kT_z}}\left(y+\sqrt{\frac{m_e}{2h\nu_0}}\frac{v_{z0}}{\eta^2}\right)\right]-Erf\left[\eta\sqrt{\frac{h\nu_0}{2kT_z}}\left(\frac{v_{z0}}{\eta^2}\sqrt{\frac{m_e}{2h\nu_0}}-y\right)\right]\right\}dy\end{aligned}, \tag{A3}$$

where

$$T_{ei} = \frac{m_e}{2k}\left(\beta_{e,x}^2+\beta_{e,y}^2+\beta_{i,x}^2+\beta_{i,y}^2\right) = \frac{m_e}{k}\left(\beta_{e,\perp}^2+\beta_{i,\perp}^2\right), \tag{A4}$$

$$T_z = \frac{m_e}{2k}\left(\beta_{e,z}^2+\beta_{i,z}^2\right), \tag{A5}$$

and

$$\eta = \sqrt{1-\frac{2T_z}{T_{ei}}}\ . \tag{A6}$$

APPENDIX B: Derivation of the recombination rate for the longitudinally cold electron and ion beam without cylindrical symmetry

For the electrons and ions with the following distribution,

$$f_e(v_e)=\frac{1}{2\pi\beta_{e,x}\beta_{e,y}}\exp\left(-\frac{v_{e,x}^2}{2\beta_{e,x}^2}-\frac{v_{e,y}^2}{2\beta_{e,y}^2}\right)\delta\left(v_{e,z}-v_{z0}\right) \tag{B1}$$

and

$$f_I(v_i)=\frac{1}{2\pi\beta_{i,x}\beta_{i,y}}\exp\left(-\frac{v_{i,x}^2}{2\beta_{i,x}^2}-\frac{v_{i,y}^2}{2\beta_{i,y}^2}\right)\delta\left(v_{i,z}\right), \tag{B2}$$

the nominator of the R.H.S. of eq. (2) becomes

$$\begin{aligned}&\int_{-\infty}^{\infty} d^3v_i d^3v_e\, f_e(v_e)\, f_I(v_i)\left|\vec{v}_e-\vec{v}_i\right|\sigma\left(\left|\vec{v}_e-\vec{v}_i\right|\right)\\ &=\frac{c_1}{(2\pi)^2\beta_{e,x}\beta_{e,y}\beta_{i,x}\beta_{i,y}}\int_{-\infty}^{\infty} dv_x dv_y\sqrt{v_x^{\,2}+v_y^{\,2}+v_{z0}^2}\,\sigma\left(\sqrt{v_x^{\,2}+v_y^{\,2}+v_{z0}^2}\right)\exp\left(-\frac{v_x^{\,2}}{2\beta_x^2}-\frac{v_y^{\,2}}{2\beta_y^2}\right),\end{aligned} \tag{B3}$$

where

$$c_1\equiv\int_{-\infty}^{\infty}\exp\left(-\mu_x\tilde{v}_{i,x}^{\,2}\right)\exp\left(-\mu_y\tilde{v}_{i,y}^{\,2}\right)d\tilde{v}_{i,x}d\tilde{v}_{i,y}=\frac{\pi}{\sqrt{\mu_x\mu_y}}, \tag{B4}$$

$$\mu_x\equiv\frac{1}{2\beta_{e,x}^2}+\frac{1}{2\beta_{i,x}^2}, \tag{B5}$$

$$\mu_y\equiv\frac{1}{2\beta_{e,y}^2}+\frac{1}{2\beta_{i,y}^2}, \tag{B6}$$

$$\beta_x\equiv\sqrt{\beta_{i,x}^2+\beta_{e,x}^2}, \tag{B7}$$

and

$$\beta_y\equiv\sqrt{\beta_{i,y}^2+\beta_{e,y}^2}. \tag{B8}$$

The denominator of the R.H.S. of eq. (2) is

$$\int_{-\infty}^{\infty} d^3v_i d^3v_e\, f_e(v_e)\, f_I(v_i)=\frac{c_1}{(2\pi)^2\beta_{e,x}\beta_{e,y}\beta_{i,x}\beta_{i,y}}\int_{-\infty}^{\infty} dv_x dv_y\,\exp\left(-\frac{v_x^{\,2}}{2\beta_x^2}-\frac{v_y^{\,2}}{2\beta_y^2}\right)=\frac{c_1\beta_x\beta_y}{2\pi\beta_{e,x}\beta_{e,y}\beta_{i,x}\beta_{i,y}}. \tag{B9}$$

Inserting eq. (B3) and eq. (B9) into eq. (2) yields

$$\alpha_r = \frac{\int_{-\infty}^{\infty} d^3v_i d^3v_e f_e(v_e) f_I(v_i) |\vec{v}_e - \vec{v}_i| \sigma(|\vec{v}_e - \vec{v}_i|)}{\int_{-\infty}^{\infty} d^3v_i d^3v_e f_e(v_e) f_I(v_i)} \tag{B10}$$

$$= \frac{1}{2\pi\beta_x\beta_y} \int_{-\infty}^{\infty} \sqrt{v_x^{\ 2} + v_y^{\ 2} + v_{z0}^2}\, \sigma\left(\sqrt{v_x^{\ 2} + v_y^{\ 2} + v_{z0}^2}\right) \exp\left(-\frac{v_x^{\ 2}}{2\beta_x^2} - \frac{v_y^{\ 2}}{2\beta_y^2}\right) dv_x dv_y$$

Eq. (B10) can be integrated in the polar system as the following:

$$\begin{aligned}
\alpha_r &= \frac{1}{2\pi\beta_x\beta_y} \int_{-\infty}^{\infty} \sqrt{v_x^{\ 2} + v_y^{\ 2} + v_{z0}^2}\, \sigma\left(\sqrt{v_x^{\ 2} + v_y^{\ 2} + v_{z0}^2}\right) \exp\left(-\frac{v_x^{\ 2}}{2\beta_x^2} - \frac{v_y^{\ 2}}{2\beta_y^2}\right) dv_x dv_y \\
&= \frac{1}{2\pi\beta_x\beta_y} \int_0^{\infty}\int_0^{2\pi} \sqrt{v^2 + v_{z0}^2}\, \sigma\left(\sqrt{v^2 + v_{z0}^2}\right) \exp\left(-\frac{v^2\cos^2\theta}{2\beta_x^2} - \frac{v^2\sin^2\theta}{2\beta_y^2}\right) v dv d\theta \quad , \\
&= \frac{1}{2\beta_x\beta_y} \int_0^{\infty} \sqrt{x + v_{z0}^2}\, \sigma\left(\sqrt{x + v_{z0}^2}\right) \exp\left(-\frac{x}{4\beta_1^2}\right) I_0\left(-\frac{x}{4\xi}\right) dx
\end{aligned} \tag{B11}$$

where

$$\beta_1^2 \equiv \frac{\beta_x^2\beta_y^2}{\beta_x^2 + \beta_y^2}, \tag{B12}$$

and

$$\xi \equiv -\frac{\beta_x^2\beta_y^2}{\beta_x^2 - \beta_y^2}. \tag{B13}$$

Inserting eq. (3) into eq. (B11) yields

$$\alpha_r = Ac \frac{h\nu_0}{m_e\beta_x\beta_y}\sqrt{\frac{2h\nu_0}{m_e c^2}}$$
$$\int_0^{\infty} \frac{1}{\sqrt{y + \frac{m_e v_{z0}^2}{2h\nu_0}}} \left[-\frac{1}{2}\ln\left(y + \frac{m_e v_{z0}^2}{2h\nu_0}\right) + \gamma_1 + \gamma_2\left(y + \frac{m_e v_{z0}^2}{2h\nu_0}\right)^{1/3}\right] \exp\left(-\frac{h\nu_0}{2m_e\beta_1^2} y\right) I_0\left(-\frac{h\nu_0}{2m_e\xi} y\right) dy \ . \tag{B14}$$

where I used $y = \frac{m_e x}{2h\nu_0}$. If I define

$$kT_1 = 2m_e\beta_1^2 = 2m_e \frac{\beta_x^2\beta_y^2}{\beta_x^2+\beta_y^2}, \tag{B15}$$

and

$$\eta = -\frac{\beta_1^2}{\xi} = \frac{\beta_x^2-\beta_y^2}{\beta_x^2+\beta_y^2}, \tag{B16}$$

eq. (B14) becomes

$$\alpha_r = Ac\frac{h\nu_0}{m_e\beta_x\beta_y}\sqrt{\frac{2h\nu_0}{m_e c^2}}$$
$$\int_0^\infty \frac{1}{\sqrt{y+\frac{m_e v_{z0}^2}{2h\nu_0}}}\left[-\frac{1}{2}\ln\left(y+\frac{m_e v_{z0}^2}{2h\nu_0}\right)+\gamma_1+\gamma_2\left(y+\frac{m_e v_{z0}^2}{2h\nu_0}\right)^{1/3}\right]\exp\left(-\frac{h\nu_0}{kT_1}y\right)I_0\left(\frac{h\nu_0}{kT_1}\eta\cdot y\right)dy\,. \tag{B17}$$